DETECTION OF HIGH RISK PLAQUES IN CORONARY ARTERIES

[1]DANTULURI SAMEELA, [2]Prof.KOMPELLA VENKATA RAMANA
[1]M.TECH SCHOLAR, [2]PROFESSOR
Department of Computer Science & Systems Engineering,
Andhra University College of Engineering (A), Visakhapatnam, India.

ABSTRACT: Intravascular ultrasound imaging of coronary arteries provides important information about coronary lumen, wall, and plaque characteristics. Quantitative studies of coronary atherosclerosis using intravascular ultrasound and manual identification of wall and plaque borders are limited by the need for observers with substantial experience and the tedious nature of manual border detection. The features like thin-gap-fibro atheroma, plaque burden and minimal luminal area are exhibiting high risk events in coronary arteries. These features prone to major cardiac events which are detected from intravascular ultrasound images. Identification of arterial locations likely to later develop such high-risk plaques may help to prevent MACE .In this paper I proposed feature extraction to extract such high risk features, automated segmentation to detect risk plaques and classification to classify the plaque and lumen area.

I. INTRODUCTION

Heart attack and stroke are the major causes of human death, almost twice as many people die from cardiovascular diseases than from all forms of cancer combined. A number of imaging modalities exist to help diagnose coronary artery disease. Among them, X-ray coronary angiography and intravascular ultrasound represents the most commonly used diagnostic tools. Intravascular ultrasound is a catheter-based technique which produces tomographic two-dimensional cross-sectional images of vessel wall architecture and plaque morphology. With intravascular ultrasound, a high-frequency ultrasound source rotates near the tip of a catheter inserted in the arterial lumen. Intravascular ultrasound morphology, determined from operator-defined borders, agrees closely with quantitative histologic determination of lumen area and mural thickness and angiographic determination of lumen size Selective coronary angiography provides projection X-ray images of contrast-filled coronary vessels and has been clinically used for several decades. While it provides detailed images of vessel lumen, it offers no information about the coronary wall. Intravascular ultrasound is a relatively new technique that offers image information that is complementary to that provided by angiography. The IVUS imaging generates cross-sectional images of the lumen, plaque, and vessel wall. Consequently, it facilitates analysis of atherosclerotic plaque composition. Considering the large number of images resulting from an IVUS study, automatic segmentation of the vessel wall is relevant to support diagnosis and interventional procedures. State-of-the-art methods can be classified into two main categories, being based on either image series or a single slide. Both fully and semi-automatic strategies can be found in each of these groups. Developing methods for vessel wall segmentation and plaque assessment in IVUS images is challenging due to the presence of speckle noise, artefacts and different imaging characteristics such as the variety of resolutions. Each of the existing solutions focuses on specific image features to capture appropriate information, and some of them are recurrently considered by different authors. Noise-reduction filters such as nonlinear filtering and anisotropic diffusion were previously applied to IVUS images for lumen–intima and media–adventitia segmentation. Textural analysis is frequently used for plaque characterization and also to differentiate arterial tissues

II. MATERIALS

In the materials 61 patients fulfilling inclusion criteria were selected from a database. The dataset contains 234 compressed images of size 384×384. These images are acquired using Si5 imaging system equipped with a 20MHz Eagle Eye catheter. Manual annotations of the luminal boundary and the media–adventitia interface are available for each image. In this study, a subset *S* of 149 images, without artefacts, shadows, bifurcations or side vessels, was selected. For the proper assessment of the learning algorithm, the set *S* was separated into a Training–validation set, containing 107 images from seven studies, and a test set, containing 42 images from three studies. For the model adjustment step, the training–validation set was split using fivefold cross-validation to prevent over fitting. Each pixel of the image was labelled using the annotations of the luminal boundary or lumen–intima and media–adventitia interfaces. The pixels within LI were labelled as lumen, and the pixels outside MA were labelled as Background.

III. METHODS

The problem of identifying the arterial wall was modelled as two different characterization problems. First, different features were evaluated to distinguish between lumen/no lumen, so that the lumen–intima interface can be estimated as the border between those two regions. A separate feature set was retrieved to distinguish between background/no background, so the media–adventitia interface can be similarly assessed by taking the frontier between these other regions.

The project includes following steps.

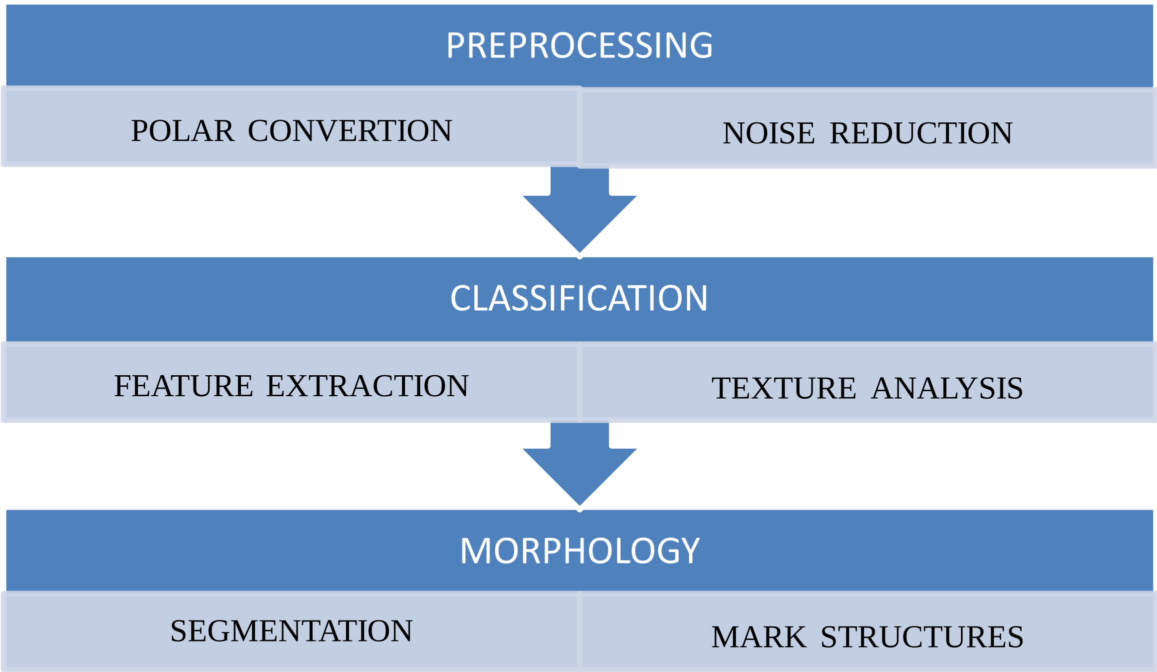

a. PREPROCESSING

Preprocessing step includes the following sub steps **POLAR CONVERTION** and **NOISE REDUCTION**

POLAR CONVERTION: IVUS images were transformed to polar coordinates since it is useful to eliminate the empty regions corresponding to the corners and the catheter area, which also facilitates arterial tissues segmentation, due to their concentric disposition As the number of transducers in IVUS systems is usually a power of two, the sampling was performed using an angle increment of 0.703◦, to obtain a lateral resolution of 512. The radial sampling step was 1 pixel, resulting in 512 × 173 sized polar images.

NOISE REDUCTION:

IVUS images are affected by speckle noise, which is characteristic of ultrasound images. Therefore, several noise-reduction filters were considered in this work. The image is convolved 25 times using a Gaussian filter with $\sigma = 0.5$. The median filter was applied 25 times using 7 × 7 windows. This size was selected due to its good behavior for window-based filters. The anisotropic diffusion was performed 6000 times with two different values of the diffusion constant $\boldsymbol{K}$: $\boldsymbol{K} = 0.013$ homogenizes lumen preserving LI, but it does not reduce noise in plaque or background; and $\boldsymbol{K} = 0.023$, which homogenizes plaque and background, preserves MA but smooth's LI. A number of specialized filters for speckle noise reduction have been recently proposed. The detail-preserving anisotropic diffusion is a DE speckling filter based on the Speckle Reducing Anisotropic Diffusion which incorporates a model of the noise within the anisotropic diffusion. For the estimation of the coefficient of noise variation, the mode of local coefficients of variation C was applied on 5 × 5 windows, as the authors recommend. The step size was set to 0.2 and the filter was applied 1000 times since those parameters showed good homogenization of the lumen, the plaque and the background

After conversion of Cartesian to polar image and noise reduction images are following.

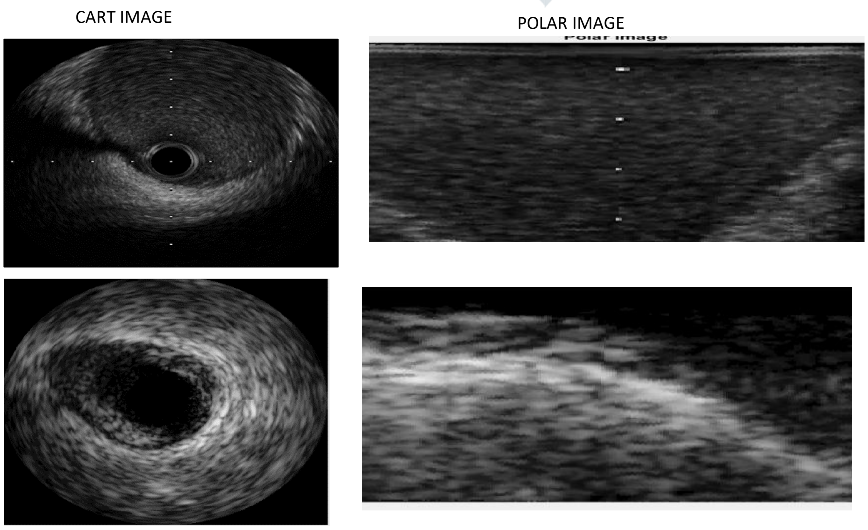

b. CLASSIFICATION:

The step classification includes mainly two steps **FEATURE EXTRACTION** and **TEXTURE ANALYSIS**

FEATURE EXTRACTION: Several approaches were proposed in the literature for feature extraction in IVUS images, depending on the region of interest to be segmented or characterized. Two main groups of features were recognized: image filters, which homogenize and/or enhance certain regions and edges; and textural features, which characterize information of the heterogeneity of the image.

Texture features includes Haralick's textural descriptors are based on grey level co-occurrence matrices, and they have been previously applied for IVUS segmentation and plaque classification. The co-occurrences of the intensities in the images were extracted from 15 × 15 windows with two different configurations of distance and orientation angles between pixels: N–S–E–W with $d = 1$ and N–S with $d = 1$ and $d = 2$. Image intensities were down sampled to 50 grey levels before computing the GLCMs, to reduce the computational cost. The calculated measures are the angular second moment, contrast, variance, inverse difference moment and entropy. Laws' textural features are based on convolving the image with 5 × 5 kernels. These matrices are obtained by taking the outer product of all the possible combinations of five predefined one-dimensional convolution kernels. After convolving the image with each matrix, 25 measures of texture energy were obtained by assigning to each pixel the sum of the absolute values in a 5 × 5 window. Local binary patterns (LBP) are used to detect texture patterns in a circular neighborhood. The LBP rotational invariant was used with $R = [1, 2, 3]$ and the corresponding neighborhood of P.

2D Gabor filters are useful not only for detecting directional borders but also for texture analysis. 16 Gabor kernels were considered, varying the standard deviation σ and the 2D frequencies. The IVUS polar images were down sampled to a resolution of 256 ×256 pixels before computing the LBP and the Gabor features. The resulting feature map was afterwards resized to the original image.

The following plots shows about lumen classification and background classification. Red color shows plaque and blue shows lumen area.

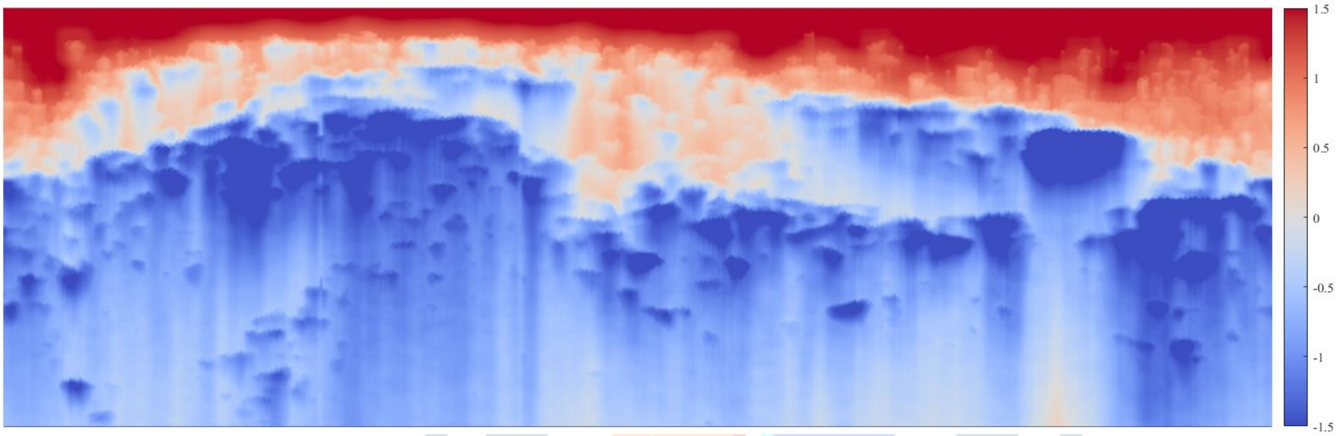

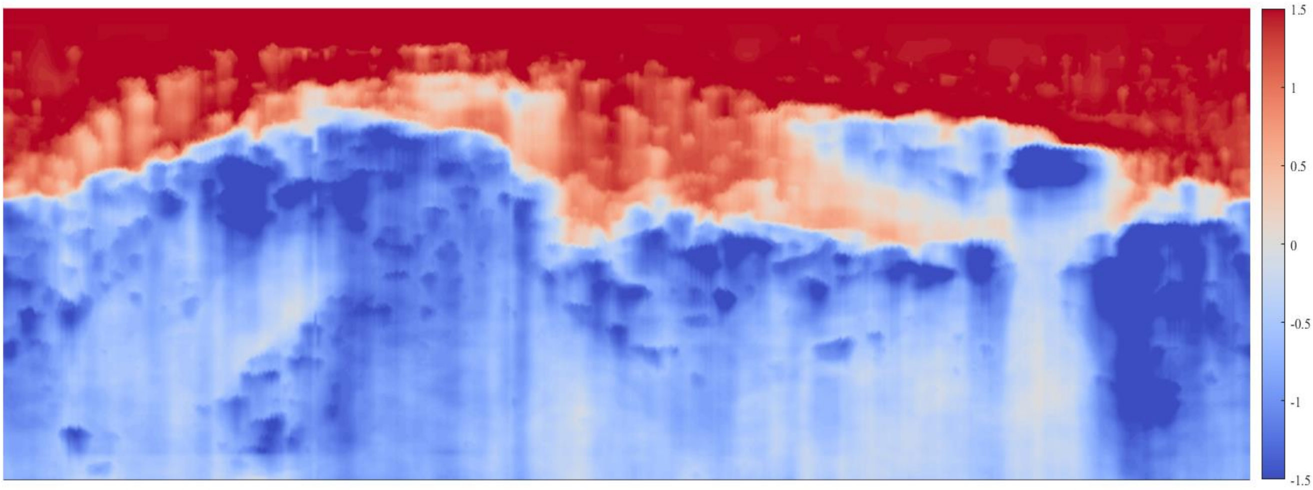

TEXTURE ANALYSIS:

Which includes support vector machine. Support vector machines (SVMs) are supervised learning models that are widely used in several applications, including data mining and image segmentation. SVMs are binary classifiers that are able to learn the optimal hyper plane that better separates two distributions of feature vectors in the feature hyperspace, according to a collection of training data. In this work, we applied SVM to characterize image pixels in the lumen/no lumen and background/no background.

Let the training set S be composed by N training samples (x_i, y_i), where $x_i \in R^M$ is the feature vector of a given pixel i, and $y_i \in \{-1,+1\}$ its corresponding true label (+1 is assigned to the class of interest and −1 to any other class).

After computing SVM on polar images the results are.

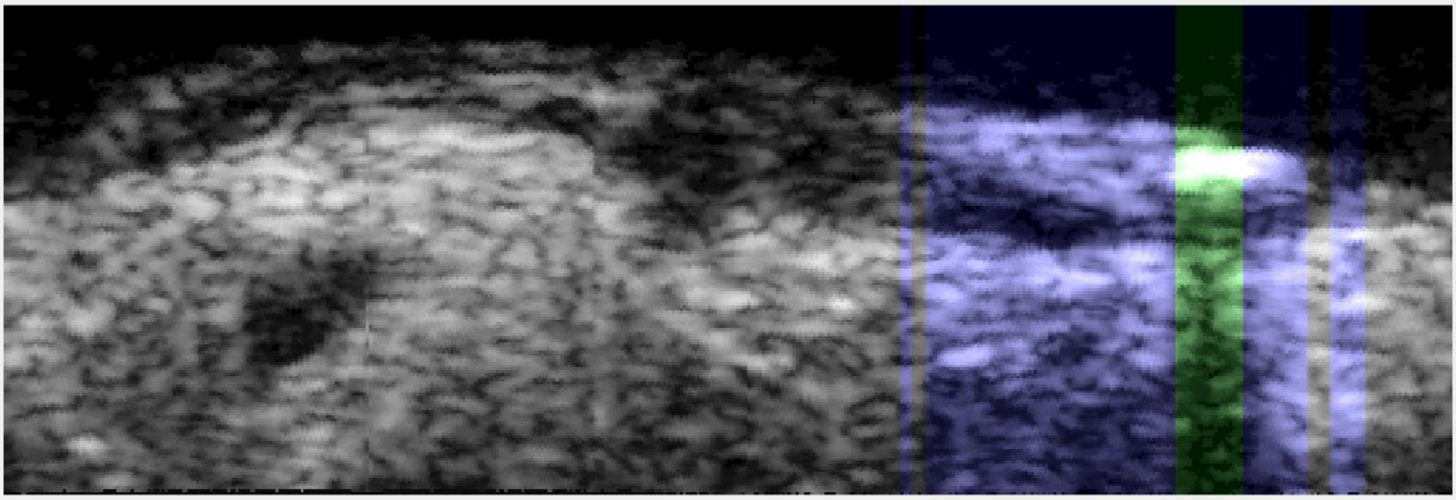

For the better result and understanding we need to convert the resultant polar image is converted into Cartesian.

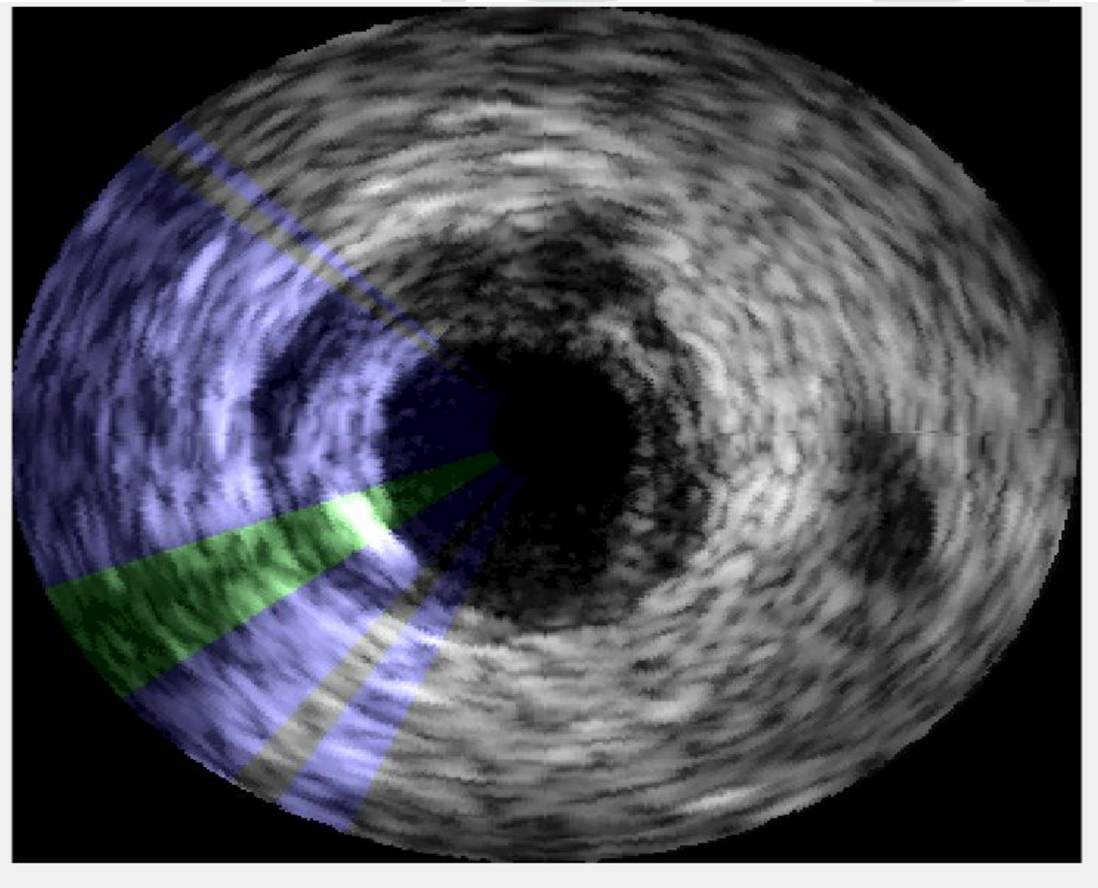

c. **MORPHOLOGY:**

Which includes segmentation and mark structures of IVUS images. In the segmentation step the polar image is converted into Cartesian.

SEGMENTATION:

Segmentation of LI and MA on IVUS is based on a highly decoupled workflow. Initially, a pixel classification belonging to Lumen and Background regions is per- formed using a linear classifier, produced by SVM. Then, morph- logical structures are detected using RF, separately from the pixel classification. A candidate edge is placed in the transition between the resulting regions. Because of the presence of structures, the edge map must be modified to erase any anomalies produced by these structures. Finally, a contour segmentation is performed using the resulting score and edge maps. LI and MA segmentations.

MORPHOLOGICAL STRUCTURES DETECTION

Columns of the polar image can present morphological structures such as bifurcations, shadows, echogenic plaques, or none of these (marked as N). Shadows are produced when the ultrasound beam cannot be propagated through a material, such as the catheter guide wire or an atherosclerotic plaque composed by calcium (calcification). Shadows prevent the observation of the arterial wall, and may cause segmentation methods to fail.

Random forest classifier

To detect the mentioned structures in polar coordinates, the intensity profile of each column was characterized using twenty two descriptors:

•mean and standard deviation
•minimum and maximum of the column total radial energy
•gray tone variance among columns
•relative gray tone
•shadow and relative shadow indicators
•median and standard deviation below maximum
•ratio between maximum and the column behind it
•Two minima and two maxima gradients
•sum of these minima and maxima gradients
•number of positive pixels using Otsu's thresholding
•slope, intercept and loss of a linear fitting

Random Forest was selected to classify each column using the listed descriptors, based on its ability to deal with multiclass and imbalanced problems in association with Random Undersampling.

SHADOW INDICATORS

Two measures related to the cumulative grey level were taken into account, namely shadow sh and relative shadow sr, defined by

$$sh(x,y) = 1/NrNc \sum_{ys=y}^{Nr} BI(x,ys)$$

And

$$sh(x,y) = 1/NrNc \sum_{ys=y}^{Nr} BI(x,ys)$$

Where BI is a binary image thresholding I with a threshold $TH = 14$, and Nr and Nc are the height and the width of the polar image, respectively.

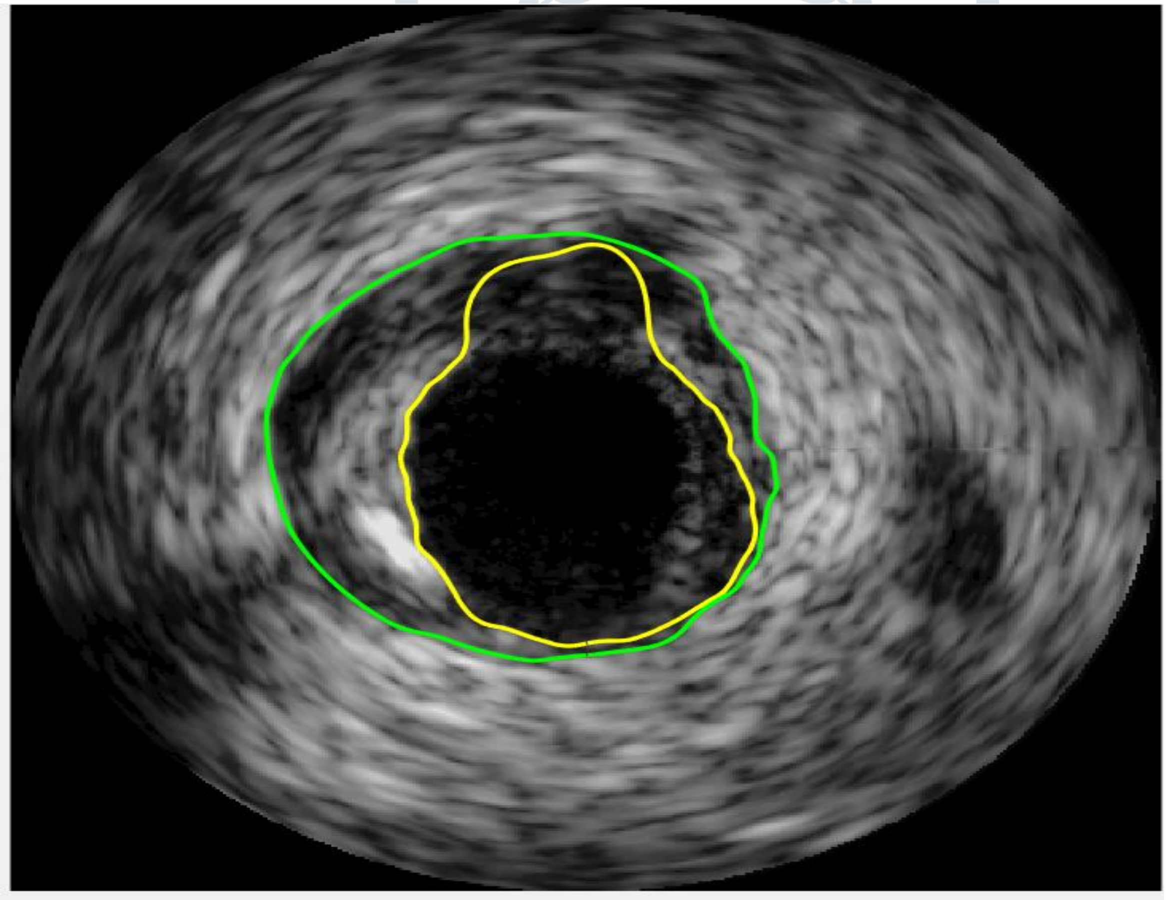

IV. **CONCLUSION**

A fully-automatic method for vessel wall segmentation in 20 MHz IVUS images was presented. It was assessed that the detection of echogenic plaques, bifurcations and shadows, and the proper modification of the layers classifications improves state-of- the-art results. As classification modules are based on machine- learning techniques, such as Support Vector Machines and Random Forest, they can be improved by using a larger dataset of IVUS images.

V. **REFERENCES**

1) M. Sonka, X. Zhang, M. Siebes, M. S. Bissing, S. DeJong, S. M. Collins, and C. R. McKay, "Segmentation of intravascular ultrasound images: A knowledge-based approach," *IEEE Trans. Med. Imag.*, vol. 14, pp. 719–732, Aug. 1995.
2) X. Zhang, C. R. McKay, and M. Sonka, "Image segmentation and tissue characterization in intravascular ultrasound," *IEEE Trans. Med. Imag.*, vol. 17, pp. 889–899, 1998.

3) L. Zhang *et al.*, "Simultaneous registration of location and orientation in intravascular ultrasound pullbacks pairs via 3D graph-based optimization," *IEEE Trans. Med. Imag.*, vol. 34, no. 12, pp. 2550–2561, Dec. 2015.

4) D. Y. Chong *et al.*, "Robustness-driven feature selection in classification of fibrotic interstitial lung disease patterns in computed tomography using 3D texture features," *IEEE Trans. Med. Imag.*, vol. 35, no. 1, pp. 144–157, Jan. 2016.

5) T. Torheim *et al.*, "Classification of dynamic contrast enhanced MR images of cervical cancers using texture analysis and support vector machines," *IEEE Trans. Med. Imag.*, vol. 33, no. 8, pp. 1648–1656,aug. 2014.